Advcanced Physics Lab SS19

Experiment: SQUID

(Conducted on 23.09.19 with Jiwen Guan)

Erik Bode, Damian Lanzenstiel
(Group 103)

October 2, 2019

Abstract

Contents

1 Theoretical Background

Disclaimer: The theoretical information is, if not specified otherwise, taken from the manual [?] or the S̈taatsexamen b̈y V.Bange [?].

1.1 Superconductors

In general, superconductors are materials which, if cooled below a critical temperature T_c, show the following properties:

- The resistance of the material drops to an immeasurable level
- The material behaves like a almost perfect diamagnet: Magnetic fields induce a surface current, which compensates external magnetic fields completely (Meissner-Ochsenfeld effect)
- The electrons inside the material form Cooper pairs of two electrons bound together over a distance of hundreds of angstroms.

There are two types of superconductors:

- Low temperature superconductors:
  The earliest discovered superconductors were of this type. The highest achievable critical Temperature is very low, usually requiring liquid helium cooling. E.g. Nb_3Ge with $T_c = 23.2\,\mathrm{K}$. Below a critical H_c field strength, magnetic fields do not penetrate the material beyond a few hundred nanometres.
- High temperature superconductors:
  With this type, the critical temperature is higher. The highest temperature is $T_C = 138\,\mathrm{K}$ with $Hg_{12}Tl_3Ba_{30}Ca_{30}Cu_{45}O_{125}$. This has the advantage that liquid nitrogen can be used as a coolant. There exist two critical magnetic field strengths, H_{c1} and H_{c2}. Below H_{c1}, the magnetic field is completely forced out of the material. Between both temperatures, magnetic flux-strings are forming inside the material which are normal conducting and enclosed by an eddy current.

1.2 BCS Theory

The BCS theory (Bardeen, Cooper, Schrieffer, 1957) explains many of the superconductor properties.

The lattice structure deforms in the orbit of an electron, since the nuclei needs a certain time, in the order of the inverse of the Debey frequency $\omega\mathrm{D}(T \approx 10^{-13}\mathrm{s})$, to return to its initial location. This results in a weak positive polarization behind the considered electron, which attracts another electron over long distances, i.e. after an almost complete weakening of the repulsive Coulomb interaction. In theoretical solid state physics, the formation of a Cooper pair is described as follows: Electrons are fermions, i.e. each quantum mechanical state is occupied only once, except for two electrons with opposite spin. At low temperatures almost all states are now filled up to the Fermi energy E_F, above which the population density drops drastically towards 0. This results in a high probability of two electrons with antiparallel impulses to be found, which favours the formation of a Cooper pair. It is also said that even relatively weak interactions lead to bound states. These combined spin 1/2 systems then have total spin 0 and behave like bosons. According to the Bose statistics, any number of bosons can occupy a state, so there is no limit for the creation of Cooper pairs . And the material is now in a superconducting state. The bosonic behaviour of the Cooper pairs causes the formation of a total wave function which is present in the ground state. This total wave has some consequences, like the flux quantization, resistance-free charge transport and effects at a Josephson contact. The wavelength of the bosonic wave functions is very large compared to the distances of the atomic bodies in the lattice, since the interaction between the electrons is very weak. Therefore, these or lattice oscillations are not obstacles for the Cooper pairs. Thus a resistance-free charge transport is given.

1.3 Josephson effect

The Josephson effect is the underlying principle of a Josephson junction, a core part of the SQUID sensor. The quantum mechanical phenomenon of tunnelling also occurs between two superconductors separated by a thin insulating layer. The insulation layer must not be a superconductor. This is essential for the SQUID experiment, since a magnetic field applied from the outside cannot penetrate into the superconductor (Meissner-Ochsenfeld effect), but into the insulating layer. The Cooper pairs can now tunnel into the other superconductors if phase difference $\Delta\phi = n \cdot \pi$. An current flows, without a potential difference. Also the pairs lose no energy while tunnelling, i.e. classically regarded there is no resistance. This seems paradoxical compared to the classical Ohm's law $U = R \cdot I$. Since the insulating layer is not a superconductor, magnetic fields can penetrate it. This influences the correlation of the wave functions of the tunnelling Cooper pairs, i.e. the phase difference $\Delta\phi$, which is a measurable change of the current. The tunnel current through the barrier is given by:

$$I_S = I_C \sin(\Delta\phi)$$

1.4 Quantisation of magnetic flux

The magnetic flux in the circular superconductor is quantised as

$$\oint \vec{A} d\vec{l} = \Phi_B \text{ for } \nabla \times \vec{A} = \vec{B}$$

where Φ_B is the magnetic flux inside the superconducting ring. Because all the Cooper pairs are in the BSC ground state, their wave functions have definite phase relations. This is the reason of the quantization of the magnetic flux in levels of the magnetic flux quantum Φ_0 as in

$$|\Phi_B| = n\frac{h}{2e} = n\Phi_0$$

1.5 The SQUID

The SQUID (*S*uperconducting *QU*antum *I*nterference *D*evice) is a verry precise sensor to detect changes in magnetic fields in the order of the flux quantum. The one used during the experiment is a RF SQUID, which has one Josephson junction inside the superconducting ring. A RF circuit generates an external magnetic flux Φ_{ext}. This flux induces a current in the superconducting ring to compensate the external field that Φ_{int} is zero. Since the total wave function of the Cooper pairs carrying the current must be constant inside the superconductor, the total flux Φ_{tot} can only be changed as multiples of the flux quantum. The Josephson contact shifts the phase of the total wave function. The phasse difference can be calculated as:

$$\theta_2 - \theta_1 = 2\pi n - 2\pi\frac{\Phi_{tot}}{\Phi_0}$$

A change of the external flux can not change the flux inside the superconducting ring, if the difference is smaller then Φ_0. These differences are compensated by a surface current which results in a surface flux $\Phi_S = LI_S$ that $\Phi_{tot} = \Phi_{ext} - \Phi_S$. The inductance L is dependant on the shape and material. If the change of flux is bigger then Φ_0, the superconductivity is interrupted while Φ_{int} is increasing. When the superconducting state is established again, the remaining flux difference smaller then Φ_0 is compensated as above.

For superconductors with a Josephson junction this is also true, although here the external magnetic field necessitates the flux quantization inside the superconductor. This results in a more complex behaviour, when $I_S = I_{S,max}\sin(\theta_2 - \theta_1)$:

$$\Phi_{tot} = \Phi_{ext} + LI_{S,max}\sin\left(2\pi\frac{\Phi_{tot}}{\Phi_0}\right)$$

2 Analysis

2.1 The Conductor Loops

To calculate the B_z value and the dipole moment p, there are two different way. The first one is to calculate the theoretical magnetic field as well as dipole moment by using the properties of the conductor loop and the applied voltage.

Here the equation 1 was used.

$$p(R) = AI(R) = \pi r^2 I(R) = \pi r^2 \frac{U}{R} \tag{1}$$

The error is than computed using Gaussian error propagation by following equation:

$$\sigma_p = \sqrt{\left(\frac{\pi U r \sigma_r}{R}\right)^2 + \left(\frac{\pi r^2 \sigma_U}{R}\right)^2 + \left(\frac{\pi r^2 U \sigma_R}{R^2}\right)^2} \tag{2}$$

The diameter d of the loop was measured multiples times and the mean was taken to get the radius . The error of the mean was calculated using equation 3. After this the value was divided by 2 to get the radius.

$$\sigma_x = \sqrt{\left(\frac{1}{n-1}\sum_{i=1}^{n}(x_i - \bar{x})^2\right)} \tag{3}$$

The voltage was gained by measuring the two attached batteries and adding them together. The values for the different resistors were given in the manual of the experiment[?] and are noted in table 1.

$$r = (1.558 \pm 0.010)\,mm$$

$$U_{ges} = U_1 + U_2 = (1.459 \pm 0.005 + 1.494 \pm 0.005)\,\mathrm{V} = (2.9530 \pm 0.0007)\,\mathrm{V}$$

With this the dipole moment for the different Resistors was calculated and are written down in table 2.

	Resistor 1	Resistor 2	Resistor 3	Resistor 4	Resistor 5
Ω	51.47 ± 0.05	100.80 ± 0.10	300.80 ± 0.30	510.6 ± 0.5	1000.0 ± 1.0

Table 1: Different Resistors for the five conductor loop measurements.

It can now be used to compute the magnetic field B_z using equation 4.

$$B_z = \frac{\mu_0 p}{2\pi z^3} \tag{4}$$

In this equation the value z is the distance of the probe to the SQUID. This was measured by measuring the length of the kryostat from top to the probe as well as from the top to the SQUID. The difference of both is the distance from probe to SQUID. To decrease the errors the mean of multiple distance measurements were taken.

$$z = (2.65 \pm 0.12)\,\mathrm{cm}$$

The with that calculated value B_z is also in table 2.

	$p\,[\mathrm{Am}^2]$	$B_z\,[\mathrm{T}]$
R1	$(8.75 \pm 0.11) \times 10^{-7}$	$(9.4 \pm 1.2) \times 10^{-9}$
R2	$(4.47 \pm 0.06) \times 10^{-7}$	$(4.8 \pm 0.6) \times 10^{-9}$
R3	$(1.498 \pm 0.020) \times 10^{-7}$	$(1.61 \pm 0.21) \times 10^{-9}$
R4	$(8.82 \pm 0.12) \times 10^{-8}$	$(9.5 \pm 1.2) \times 10^{-10}$
R5	$(4.51 \pm 0.06) \times 10^{-8}$	$(4.8 \pm 0.6) \times 10^{-10}$

Table 2: Values of the magnetic field and the dipole moment for the five different resistors. Calculated by using equation 1 and 4

The other way to calculate the dipole moment and magnetic field was by using the measured signals of the SQUID. Here the signal shapes were fitted with the help of Pythons package `scipy.optimize` with the method `curve_fit`. Here the form given in equation 5 was used. With that the offset a, the frequency $\omega = c$ as well as the amplitude $b = \Delta V$ can be calculated.

$$f(x) = a + b\sin(cx + d) \tag{5}$$

An example of the fits can be seen in figure **??** the other ones are in the appendix.

The parameters b of the different measurements for each resistor were taken and the weighted mean of them was taken. For this mean the equation 6 and 7 were used. The values are listed in table 3.

$$\bar{x}_g = \frac{\sum_i g_i x_i}{\sum_i g_i} \qquad \text{with} \qquad g_i = \frac{1}{\sigma_i^2} \tag{6}$$

$$\sigma_{\bar{x}_g} = \frac{1}{\sqrt{\sum_i 1/\sigma_i^2}} \tag{7}$$

With these voltages the magnetic field B_z can be computed using equation 8. An similar to the calculation for the theoretical values equation 4 can be used to gain the dipole moment p.

$$B_z = F\frac{\Delta V}{s_i} \tag{8}$$

The value of F the field flux coefficient is $9.3\,\frac{\mathrm{nT}}{\Phi_0}$ and s_i is transfer coefficient. This one can be looked up in the manual[**?**]. For the conductor loops a FB-R resistance of $100\,\mathrm{k\Omega}$ was chosen which leads to a s_i value of $1900\,\frac{mV}{\Phi_0}$. The values of the calculated magnetic field and dipole moment are noted in table 3

	$p[\mathrm{Am}^2]$	$B_z[\mathrm{T}]$	$\Delta V\,[\mathrm{V}]$
R1	$(2.19 \pm 0.29) \times 10^{-7}$	$(2.356 \pm 0.007) \times 10^{-9}$	0.2407 ± 0.0007
R2	$(1.18 \pm 0.15) \times 10^{-7}$	$(1.271 \pm 0.007) \times 10^{-9}$	0.1298 ± 0.0007
R3	$(3.9 \pm 0.5) \times 10^{-8}$	$(4.17 \pm 0.08) \times 10^{-10}$	0.0426 ± 0.0008
R4	$(2.36 \pm 0.31) \times 10^{-8}$	$(2.54 \pm 0.05) \times 10^{-10}$	0.0259 ± 0.0005
R5	$(1.37 \pm 0.19) \times 10^{-8}$	$(1.47 \pm 0.06) \times 10^{-10}$	0.0150 ± 0.0006

Table 3: Measured values for the different conductor loops using the fits of the SQUID signals.

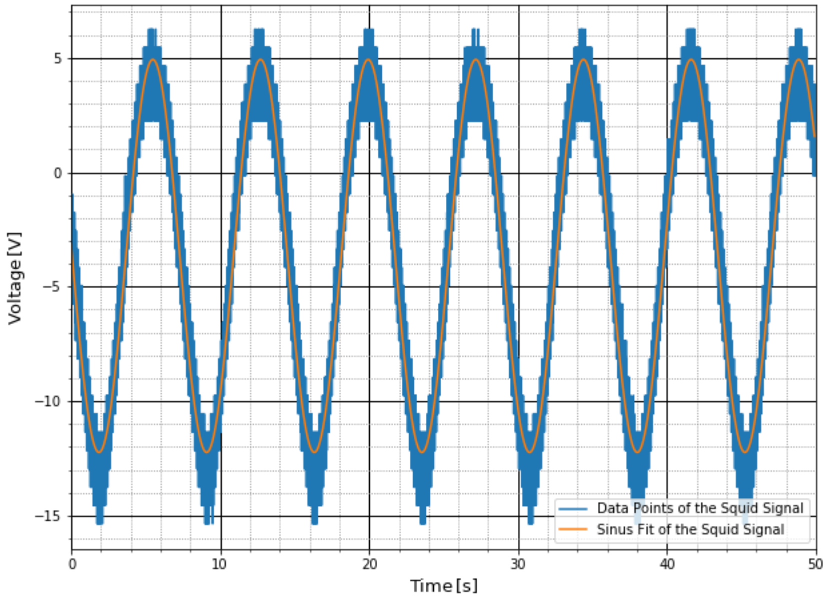

Figure 1: In blue the signal coming from the SQUID and in orange the sinus fit to the data points.

2.2 Other Samples

During the measurement other samples were tested with the SQUID. The SQUID signals were analysed in a similar way to the conductor Loops before. The sinus of the form 5 was fitted on the signal. The mean of amplitude which is parameter b was computed for the different samples and with this the magnetic field B_z and dipole moment could be calculated and can be found in table 4 in the table below.

	$p[\mathrm{Am}^2]$	$B_z[\mathrm{T}]$	$\Delta V\,[\mathrm{V}]$
Iron chips	$(1.84 \pm 0.25) \times 10^{-8}$	$(1.98 \pm 0.07) \times 10^{-10}$	0.0202 ± 0.0007
Gold lamella	$(3.2 \pm 0.4) \times 10^{-8}$	$(3.42 \pm 0.12) \times 10^{-10}$	0.0349 ± 0.0012
Magnet chips	$(7.8 \pm 1.0) \times 10^{-6}$	$(8.408 \pm 0.030) \times 10^{-8}$	8.589 ± 0.031
Stone	$(7.4 \pm 1.1) \times 10^{-10}$	$(7.9 \pm 0.5) \times 10^{-12}$	0.00081 ± 0.00005
Magnet	0.000262 ± 0.000034	$(2.814 \pm 0.014) \times 10^{-6}$	6.355 ± 0.031

Table 4: Measured and calculated values for different materials and forms of samples.

2.3 Polar Representation

For the samples and conductor loops the polar representation should be plotted. For this one period of the data points was taken. With the help of the coordinate transformation of the manual[?]:

$$x_i = |B_z| \cdot \cos(\alpha) \tag{9}$$

$$y_i = |B_z| \cdot \sin(\alpha) \tag{10}$$

Here α is the rotation angle. For the stone the polar representation can be seen in figure **??**, the rest is in the appendix.

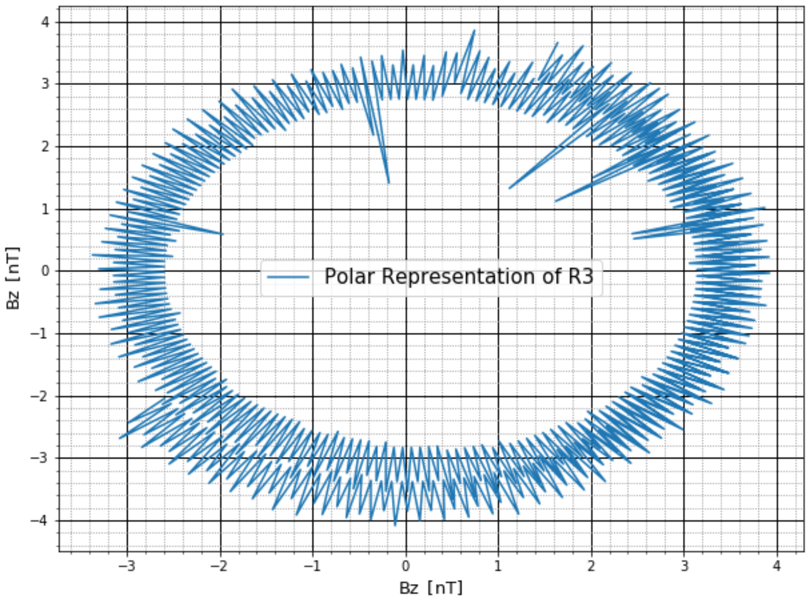

Figure 2: Polar Representation for one period of the signal coming from the R2 Conductor Loop.

3 Tabeles

List of Tables

4 Figure

List of Figures

5 Bibliograpy

References

6 Appendix

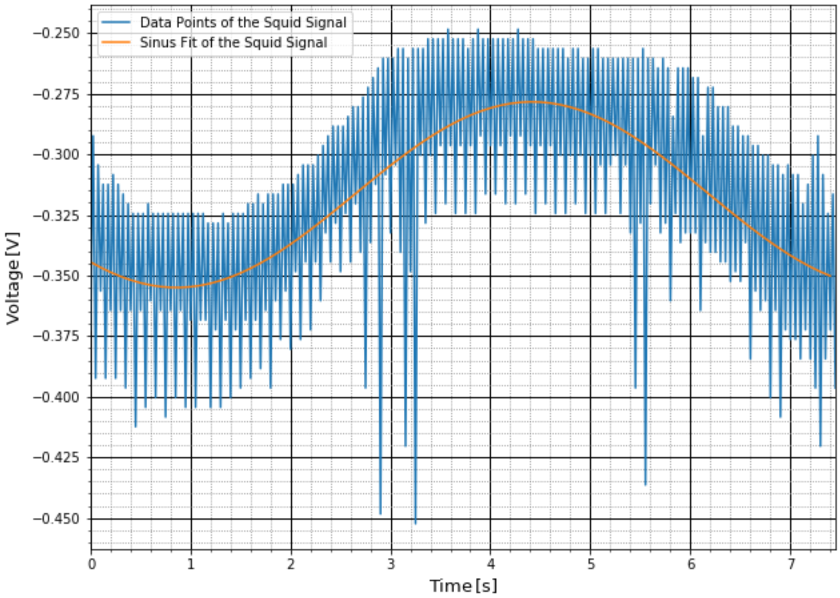

Figure 3: Plot 1 of the first conductor loop with resistor R1. The speed of the rotation here was 5. In orange is the sinus fit of the data point.

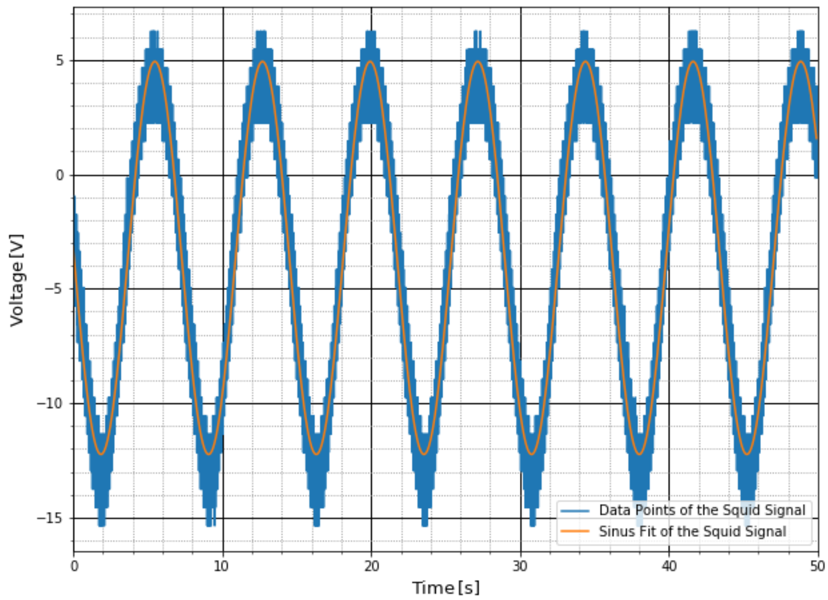

Figure 4: Plot 2 of the first conductor loop with resistor R1. The speed of the rotation here was 5. In orange is the sinus fit of the data point.

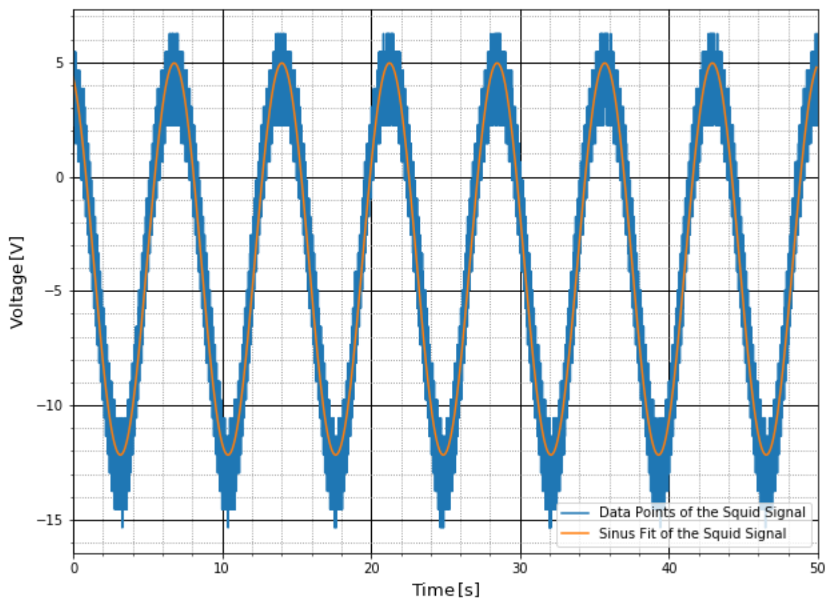

Figure 5: Plot 3 of the first conductor loop with resistor R1. The speed of the rotation here was 5. In orange is the sinus fit of the data point.

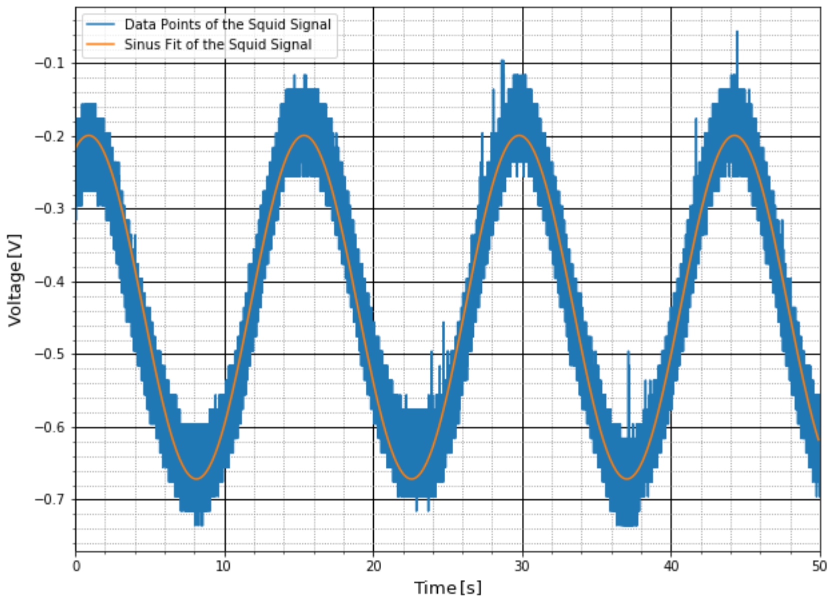

Figure 6: Plot 4 of the first conductor loop with resistor R1. The speed of the rotation here was 5. In orange is the sinus fit of the data point.

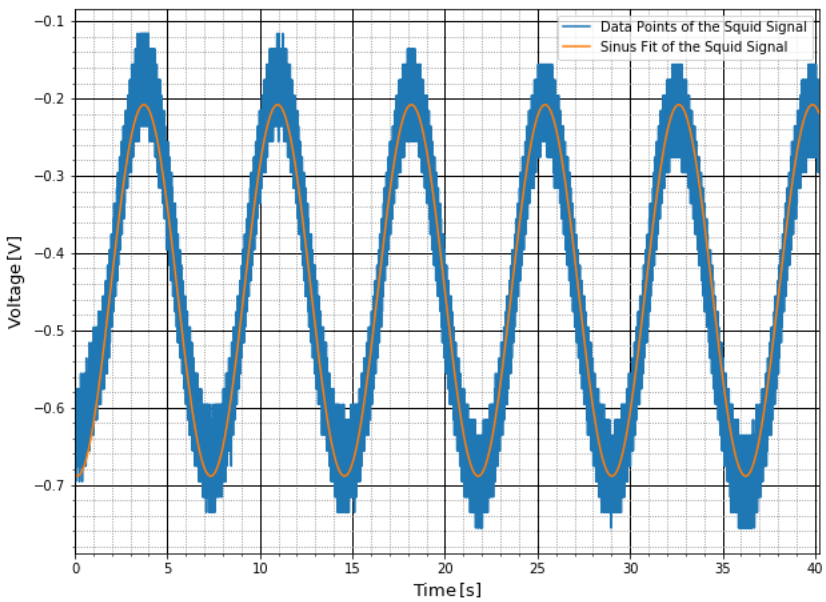

Figure 7: Plot 5 of the first conductor loop with resistor R1. The speed of the rotation here was 10. In orange is the sinus fit of the data point.

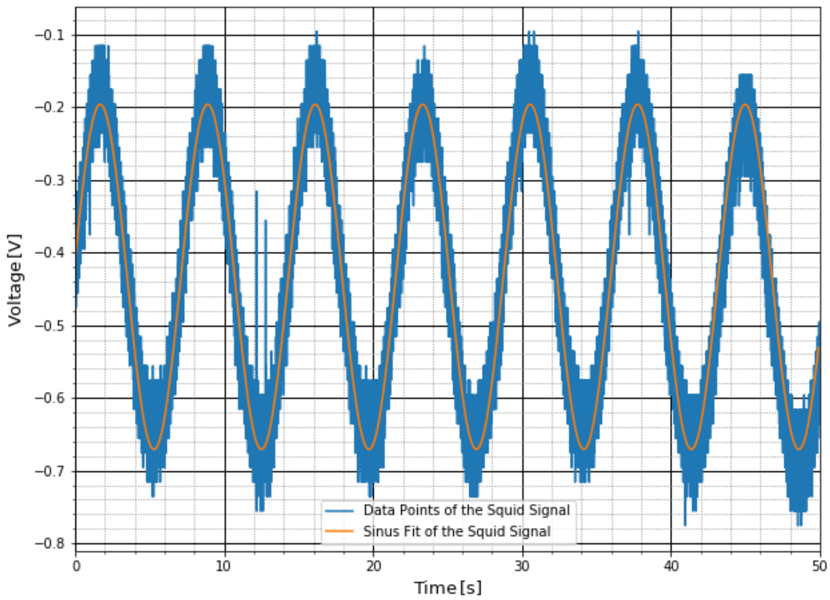

Figure 8: Plot 6 of the first conductor loop with resistor R1. The speed of the rotation here was 10. In orange is the sinus fit of the data point.

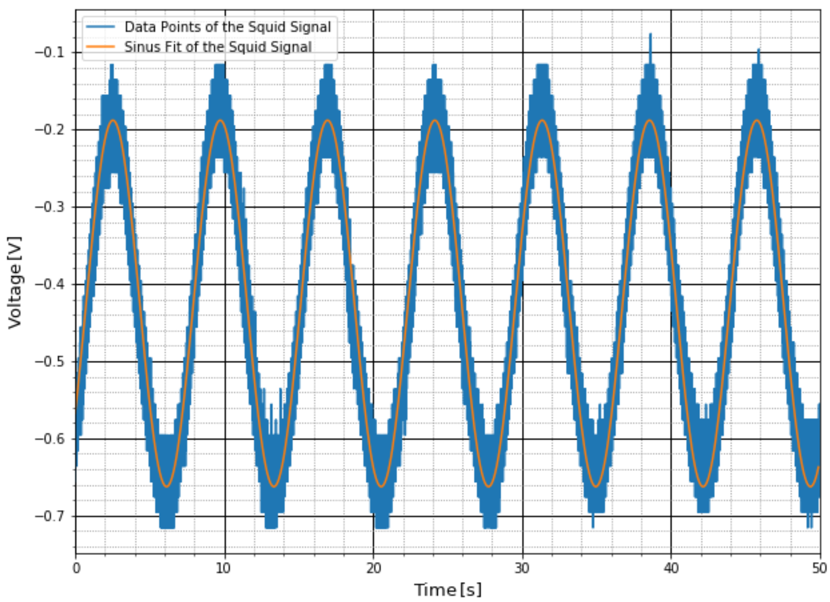

Figure 9: Plot 7 of the first conductor loop with resistor R1. The speed of the rotation here was 10. In orange is the sinus fit of the data point.

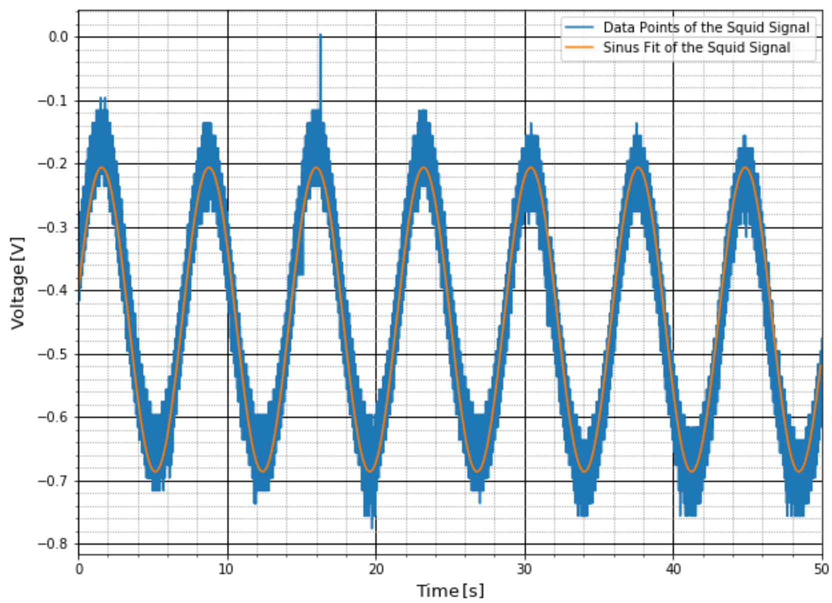

Figure 10: Plot 8 of the first conductor loop with resistor R1. The speed of the rotation here was 10. In orange is the sinus fit of the data point.

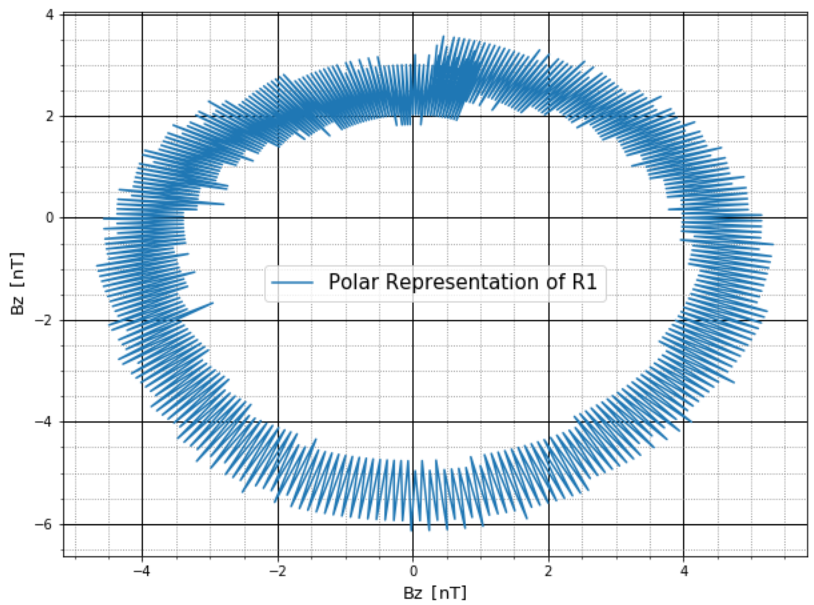

Figure 11: Polar Representation for one period of the signal coming from the R1 Conductor Loop.

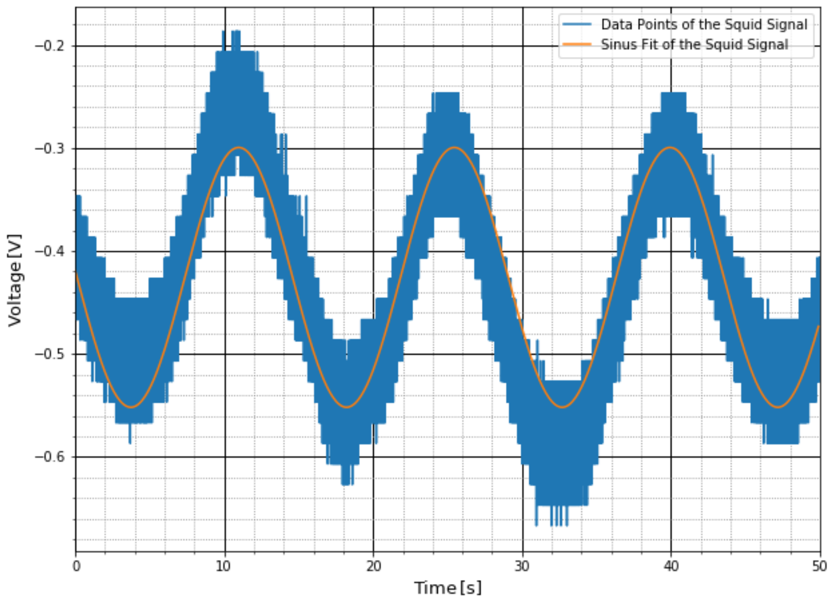

Figure 12: Plot 1 of the second conductor loop with resistor 2. The speed of the rotation here was 5. In orange is the sinus fit of the data point.

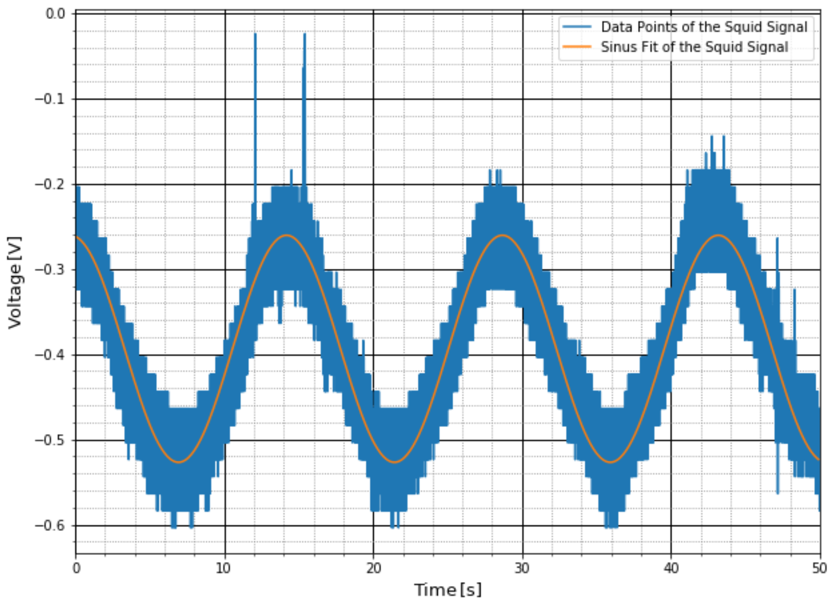

Figure 13: Plot 2 of the second conductor loop with resistor 2. The speed of the rotation here was 5. In orange is the sinus fit of the data point.

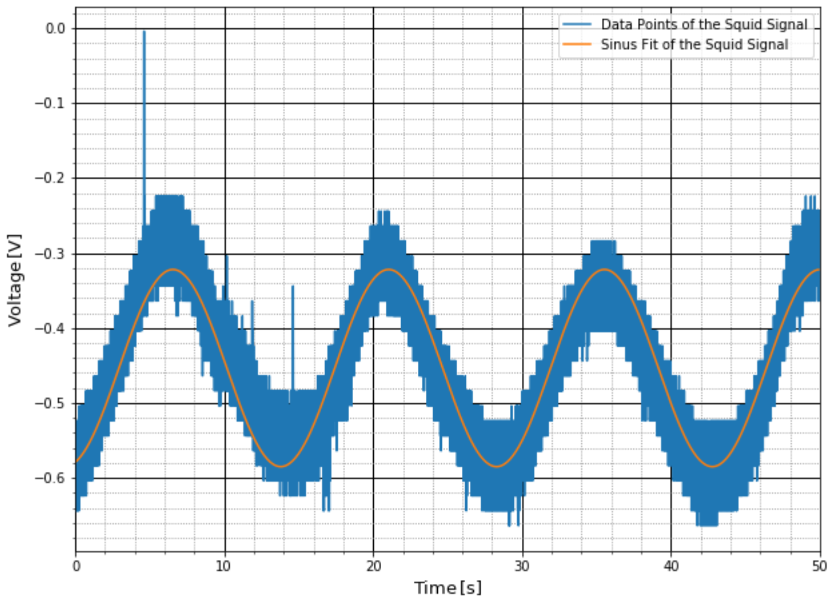

Figure 14: Plot 3 of the second conductor loop with resistor 2. The speed of the rotation here was 5. In orange is the sinus fit of the data point.

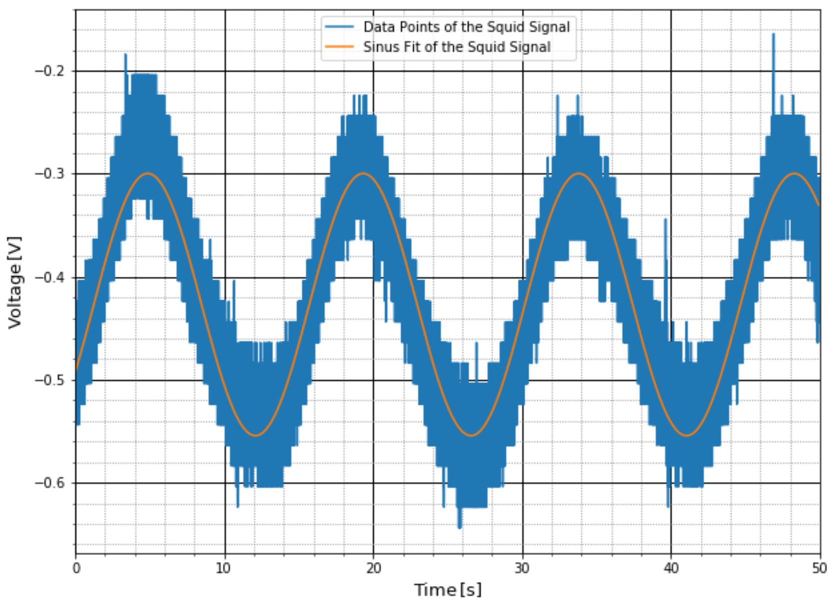

Figure 15: Plot 4 of the second conductor loop with resistor 2. The speed of the rotation here was 5. In orange is the sinus fit of the data point.

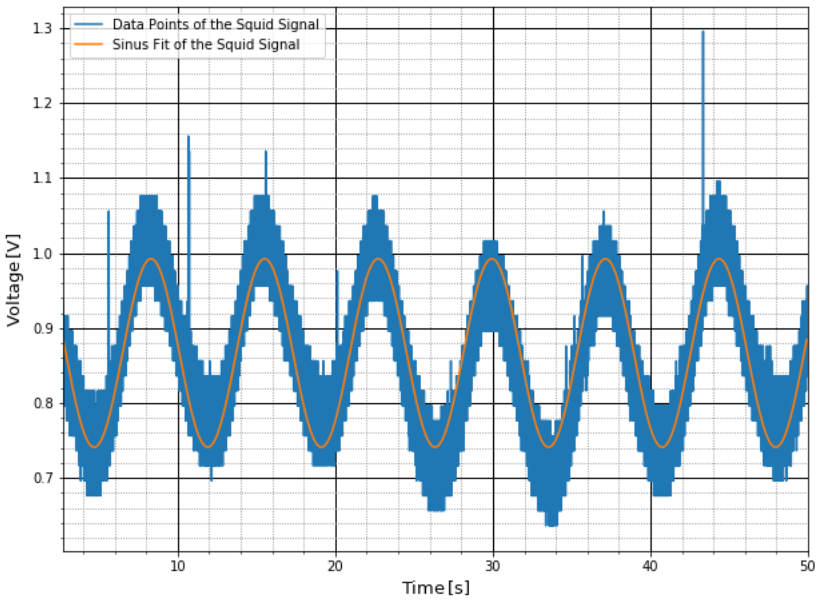

Figure 16: Plot 5 of the second conductor loop with resistor 2. The speed of the rotation here was 10. In orange is the sinus fit of the data point.

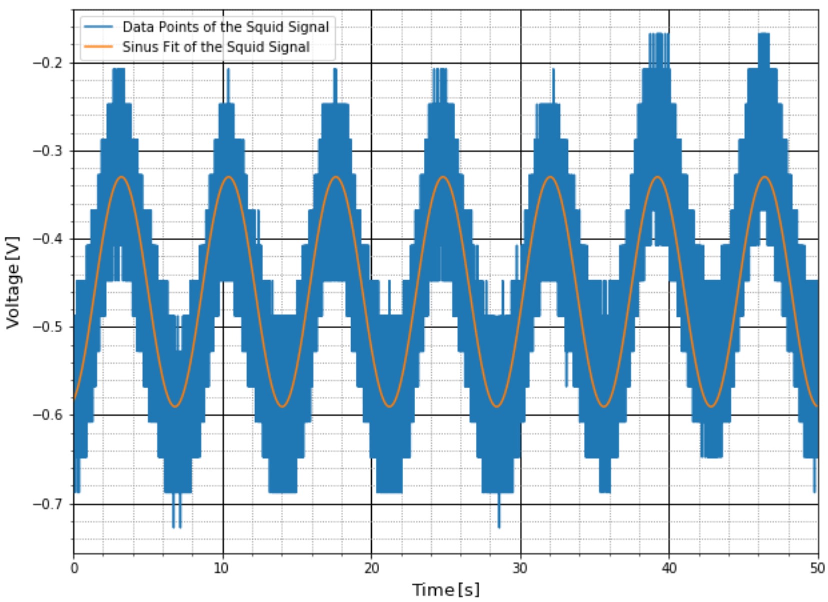

Figure 17: Plot 6 of the second conductor loop with resistor 2. The speed of the rotation here was 10. In orange is the sinus fit of the data point.

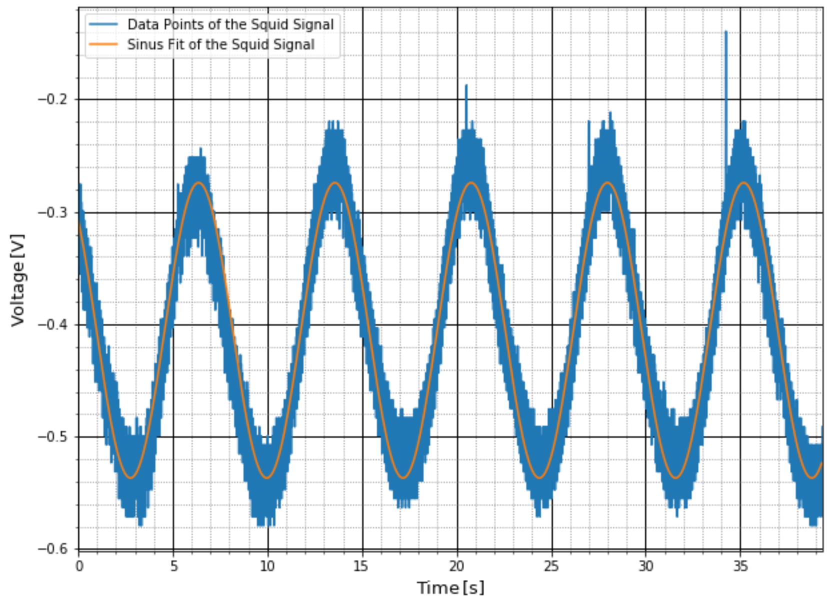

Figure 18: Plot 7 of the second conductor loop with resistor 2. The speed of the rotation here was 10. In orange is the sinus fit of the data point.

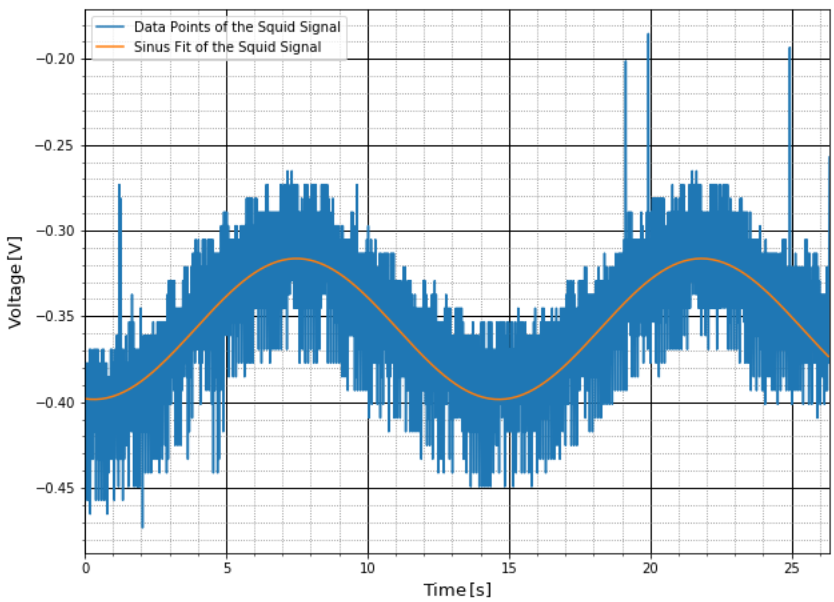

Figure 19: Plot 1 of the third conductor loop with resistor 3. The speed of the rotation here was 5. In orange is the sinus fit of the data point.

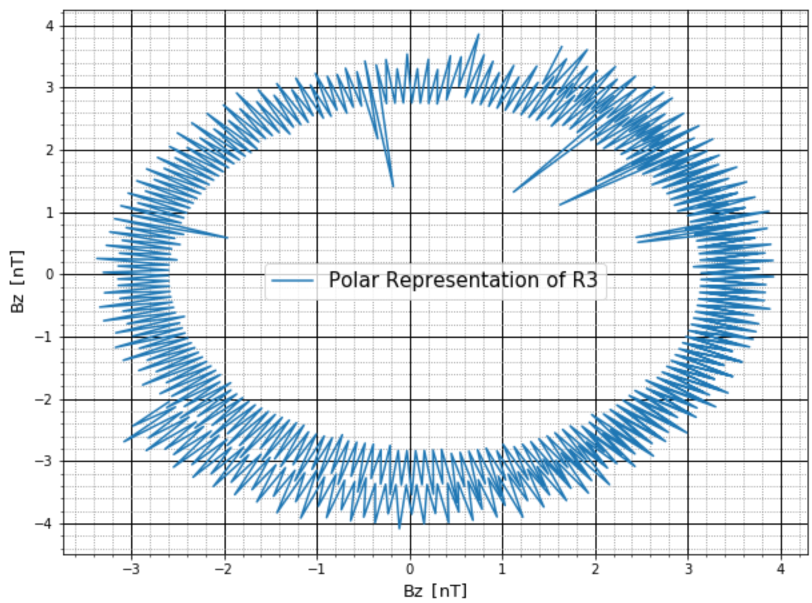

Figure 20: Polar Representation for one period of the signal coming from the R3 Conductor Loop.

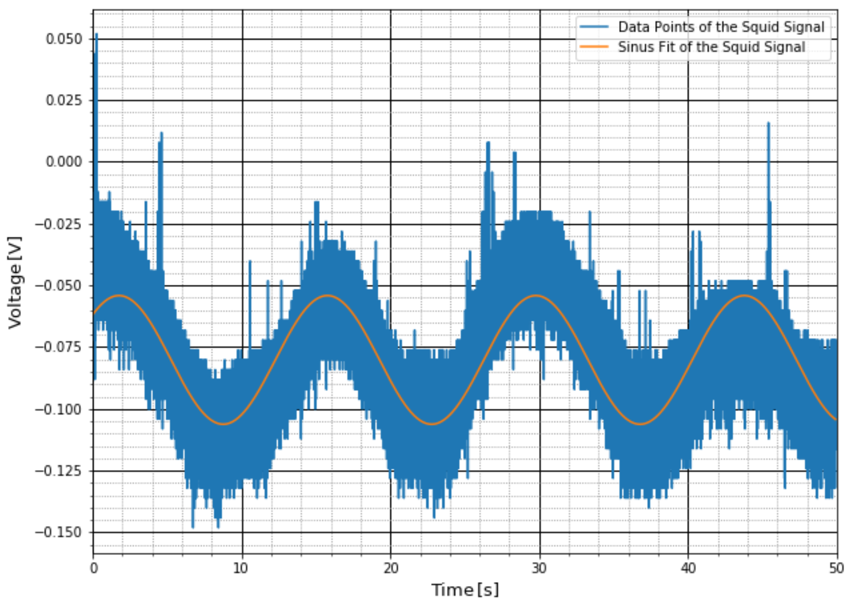

Figure 21: Plot 1 of the fourth conductor loop with resistor 4. The speed of the rotation here was 5. In orange is the sinus fit of the data point.

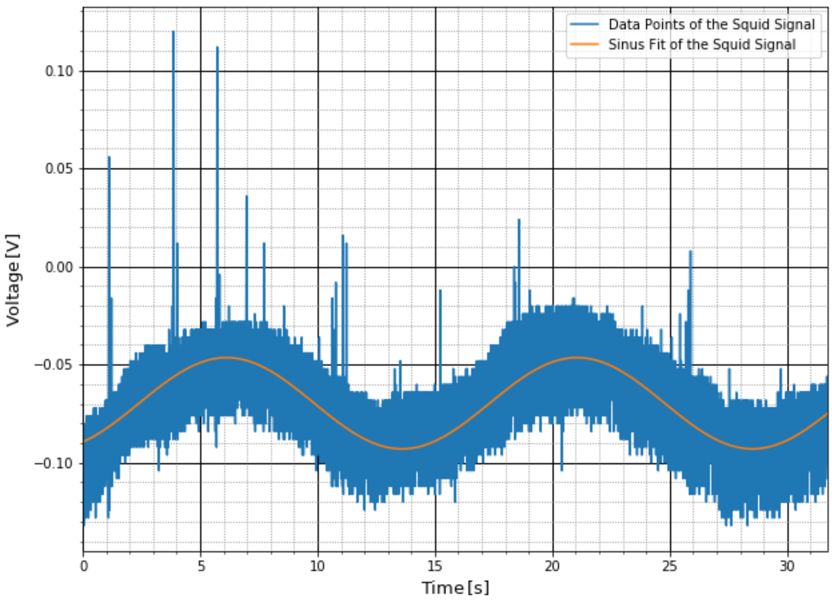

Figure 22: Plot 2 of the fourth conductor loop with resistor 4. The speed of the rotation here was 5. In orange is the sinus fit of the data point.

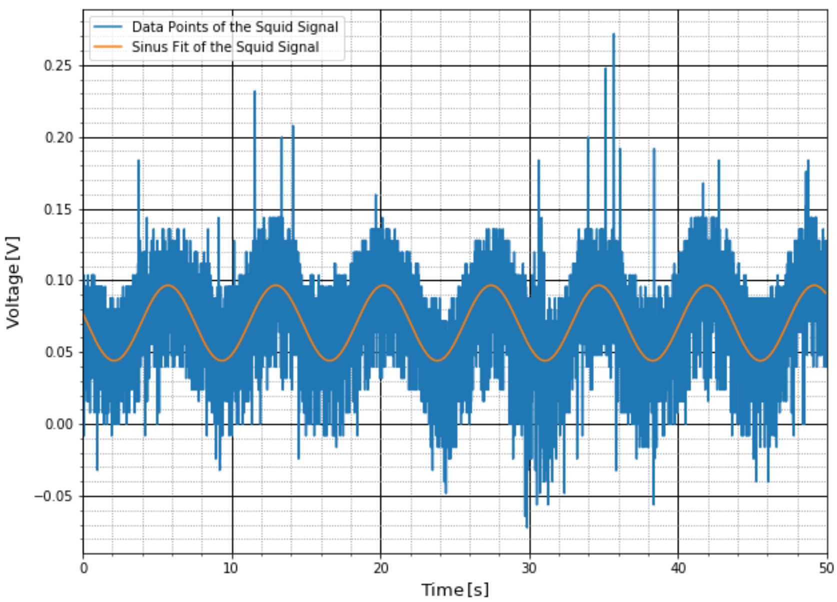

Figure 23: Plot 3 of the fourth conductor loop with resistor 4. The speed of the rotation here was 10. In orange is the sinus fit of the data point.

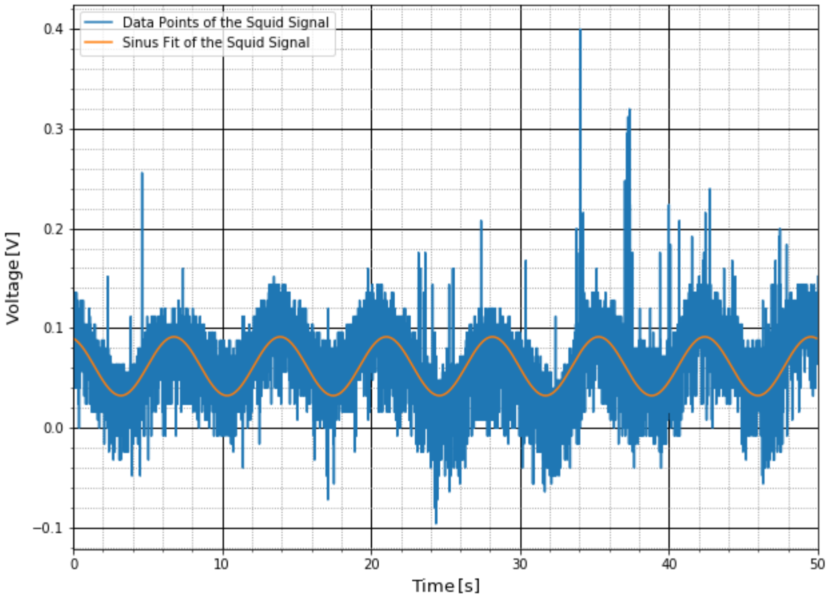

Figure 24: Plot 4 of the fourth conductor loop with resistor 4. The speed of the rotation here was 10. In orange is the sinus fit of the data point.

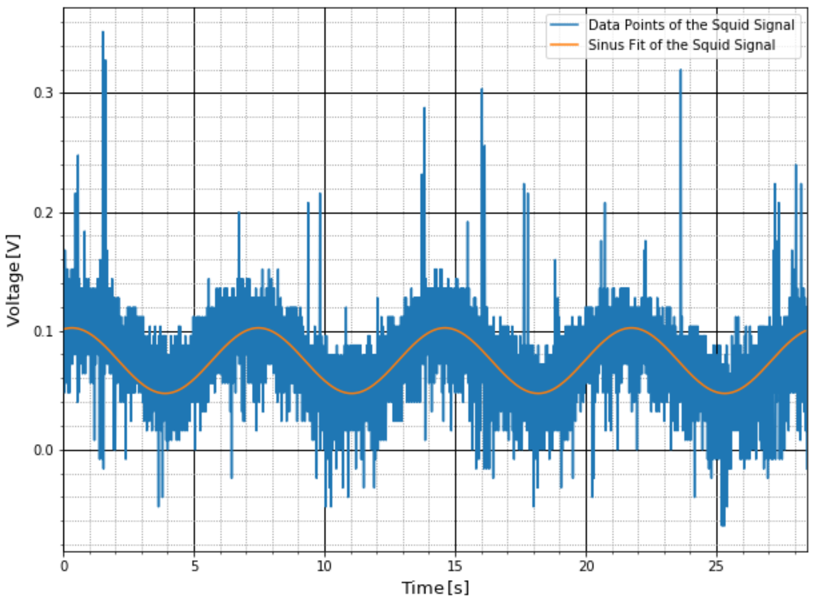

Figure 25: Plot 5 of the fourth conductor loop with resistor 4. The speed of the rotation here was 10. In orange is the sinus fit of the data point.

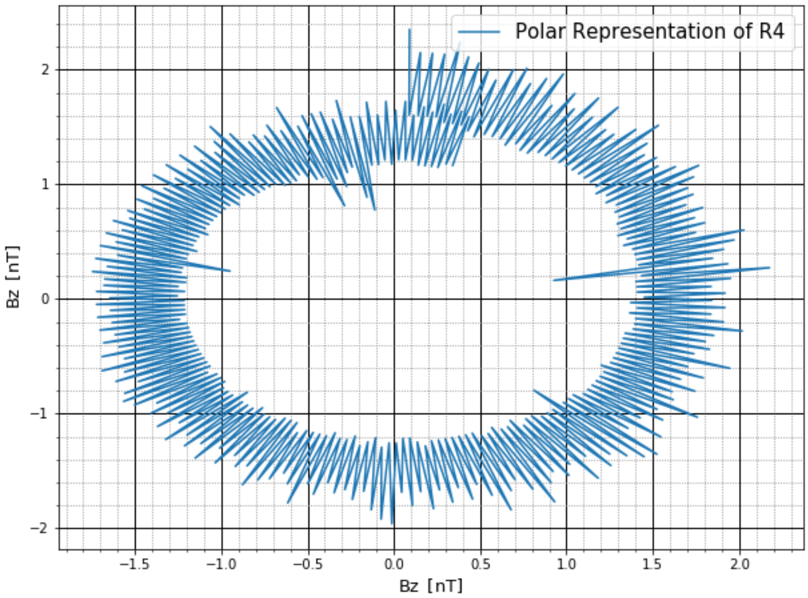

Figure 26: Polar Representation for one period of the signal coming from the R4 Conductor Loop.

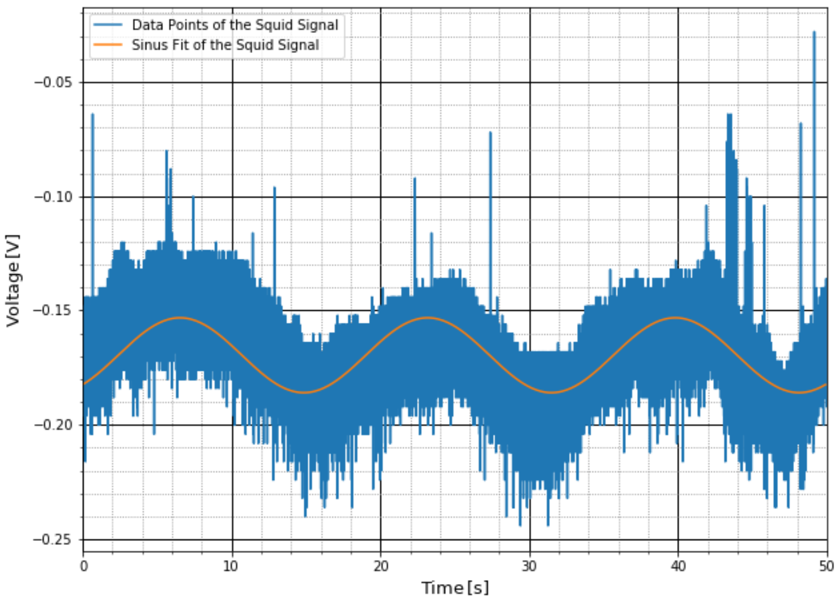

Figure 27: Plot 1 of the fifth conductor loop with resistor 5. The speed of the rotation here was 5. In orange is the sinus fit of the data point.

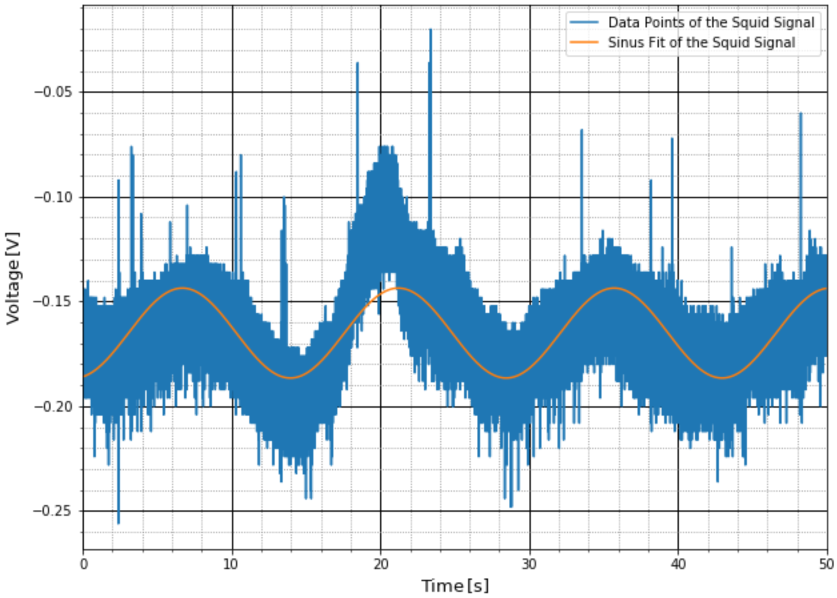

Figure 28: Plot 2 of the fifth conductor loop with resistor 5. The speed of the rotation here was 5. In orange is the sinus fit of the data point.

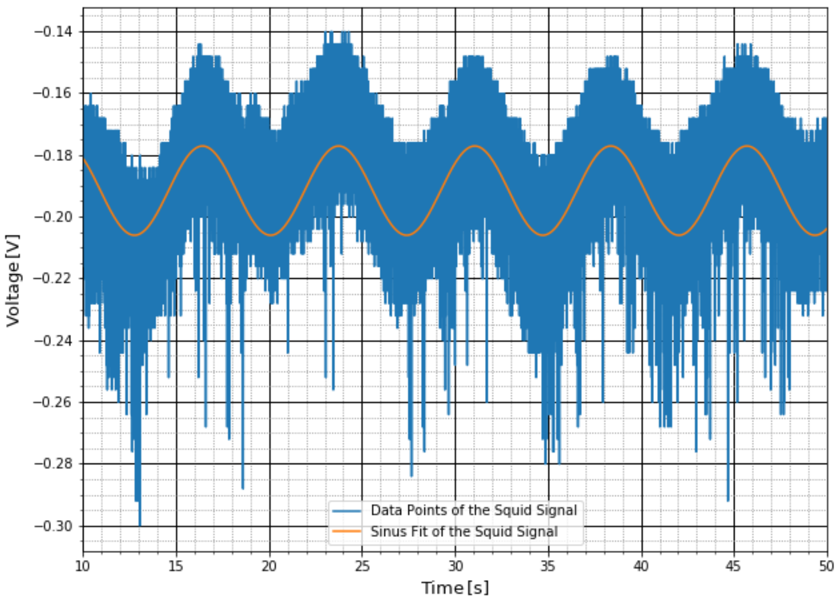

Figure 29: Plot 3 of the fifth conductor loop with resistor 5. The speed of the rotation here was 10. In orange is the sinus fit of the data point.

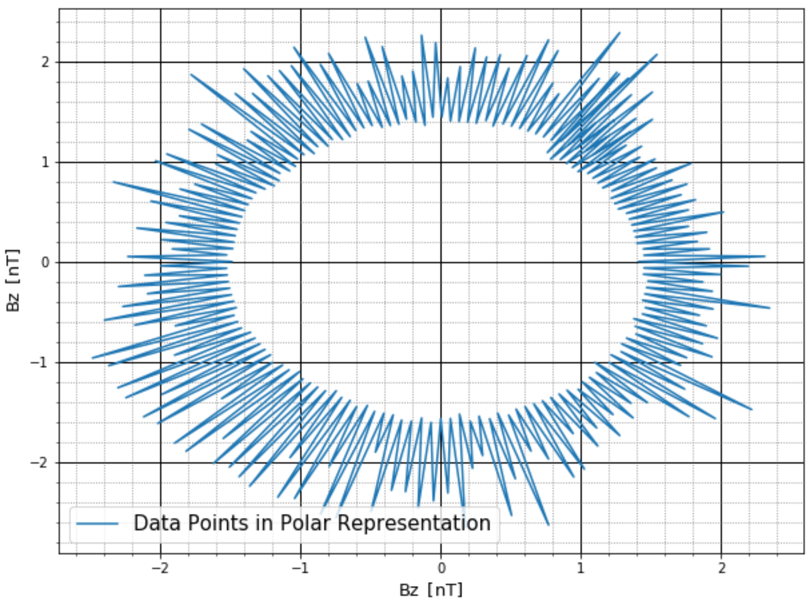

Figure 30: Polar Representation for one period of the signal coming from the R5 Conductor Loop.

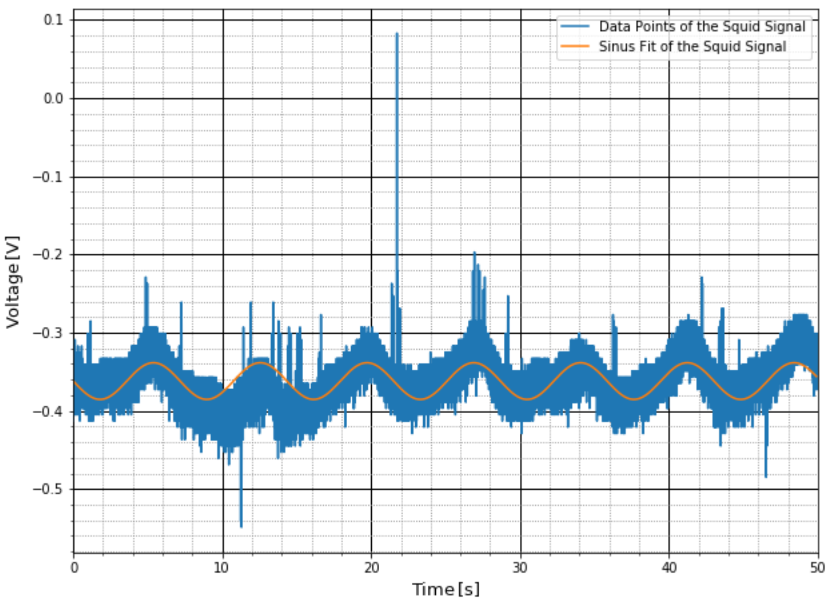

Figure 31: Plot of the SQUID signal with Iron chips as a sample.

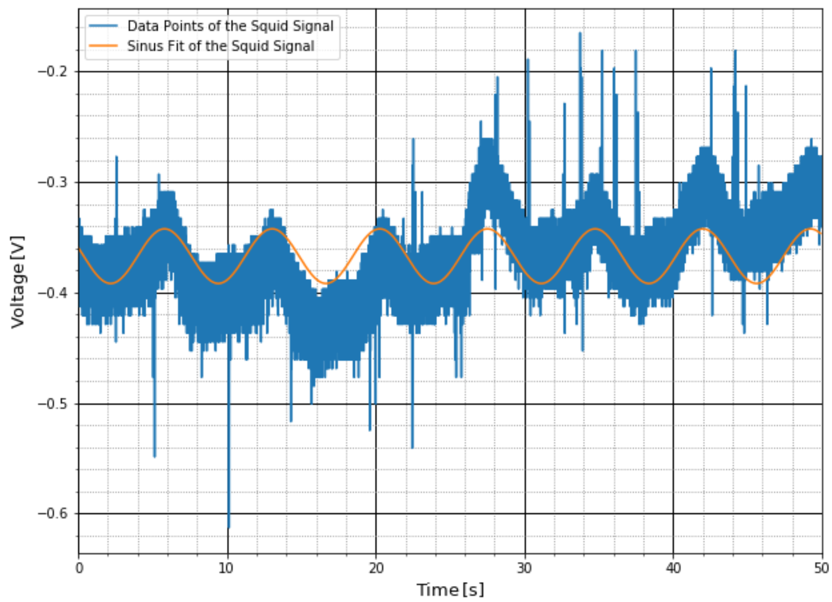

Figure 32: Plot of the SQUID signal with Iron chips as a sample.

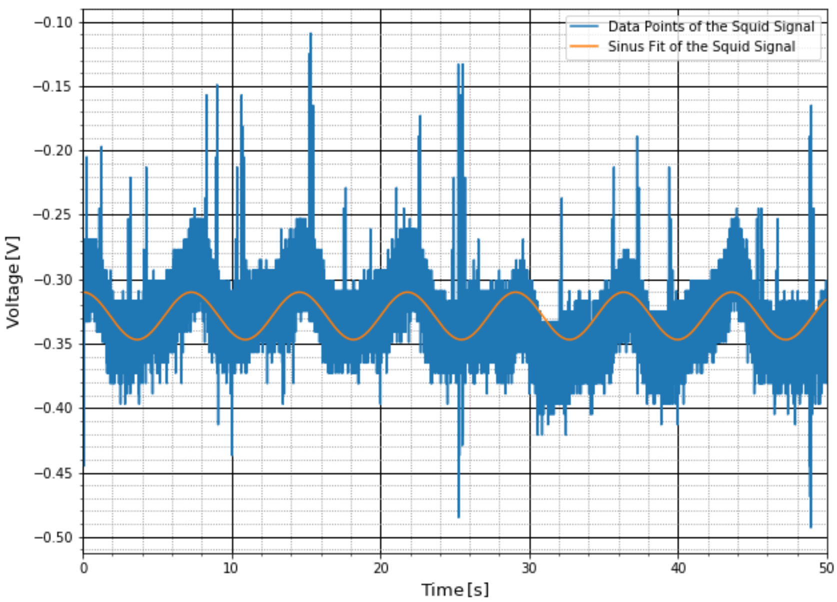

Figure 33: Plot of the SQUID signal with Iron chips as a sample.

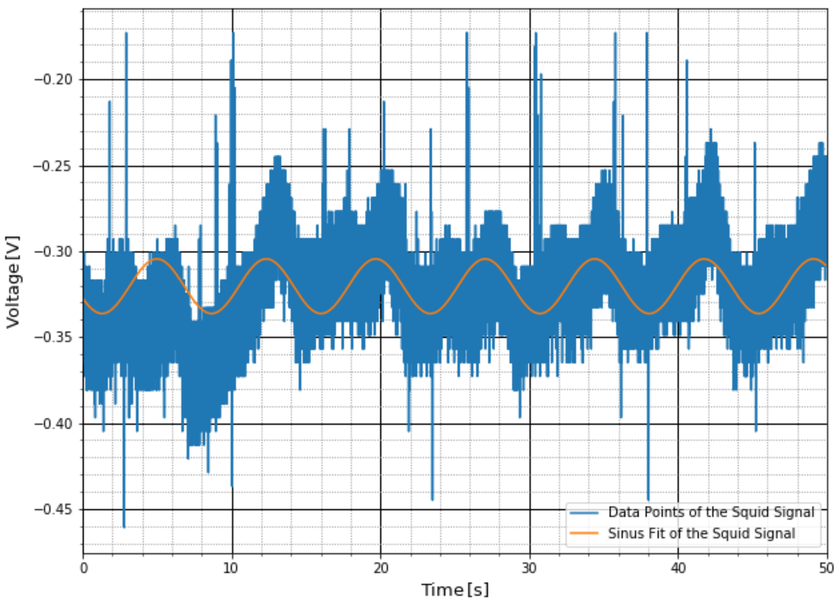

Figure 34: Plot of the SQUID signal with Iron chips as a sample.

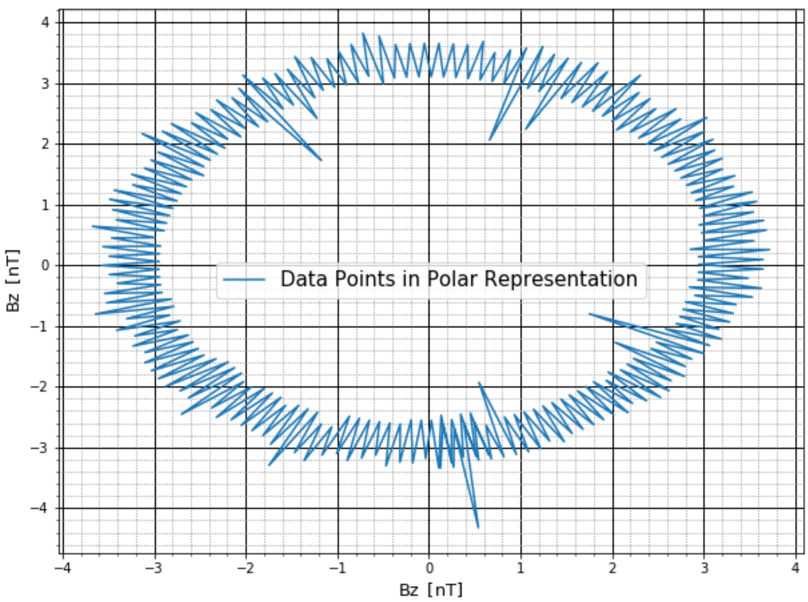

Figure 35: Polar Representation for one period of the signal coming from the iron chips.

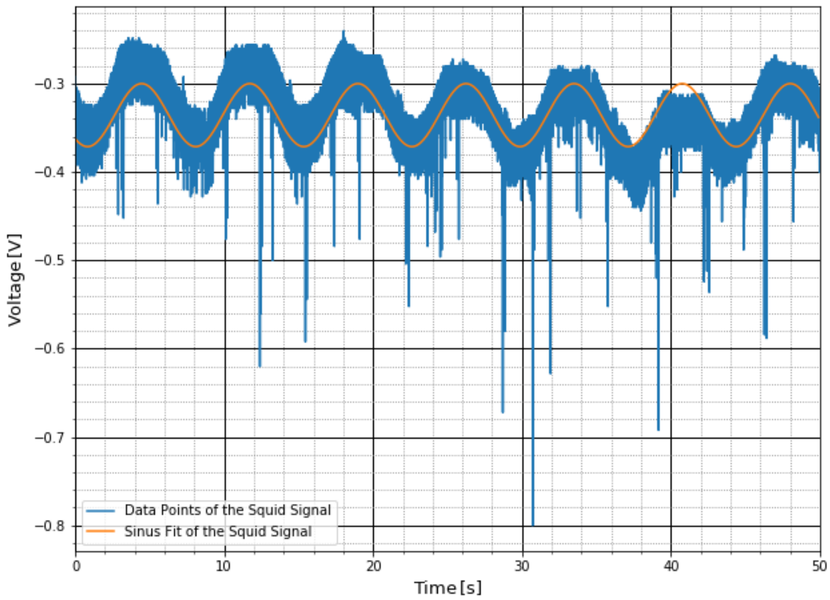

Figure 36: Plot of the SQUID signal with Gold Slide as a sample.

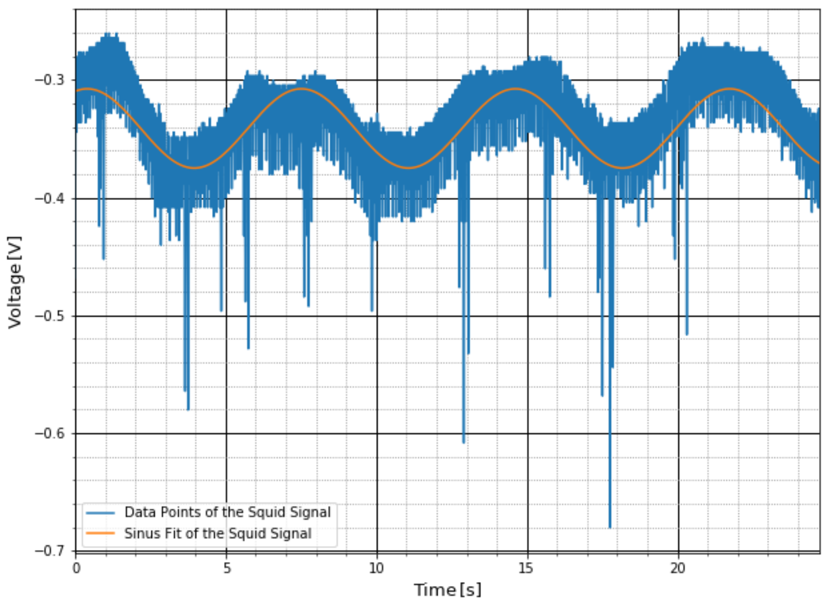

Figure 37: Plot of the SQUID signal with Gold Slide as a sample.

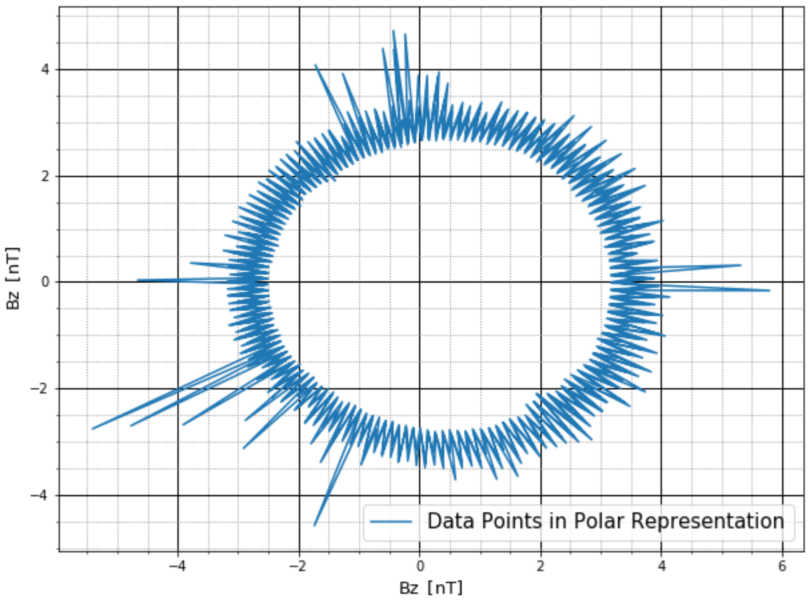

Figure 38: Polar Representation for one period of the signal coming from the gold slide.

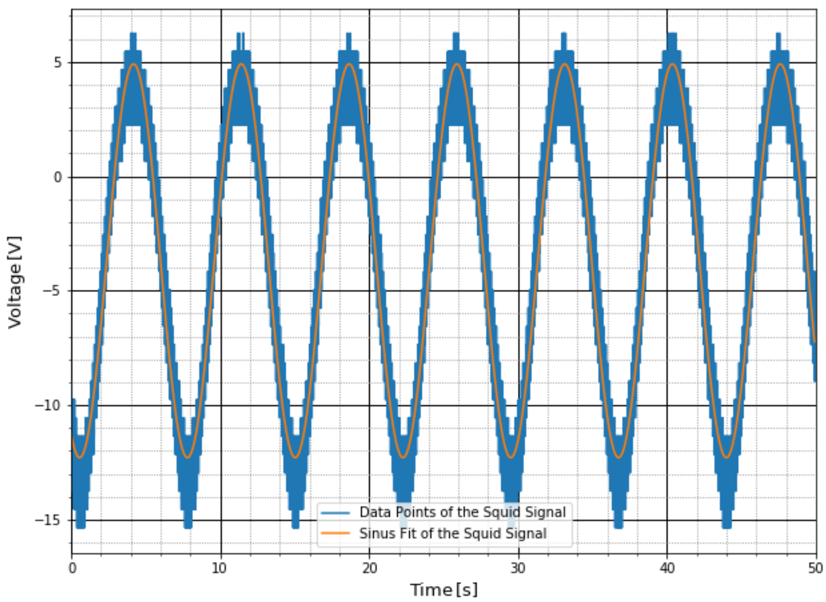

Figure 39: Plot of the SQUID signal with Magnet chips as a sample.

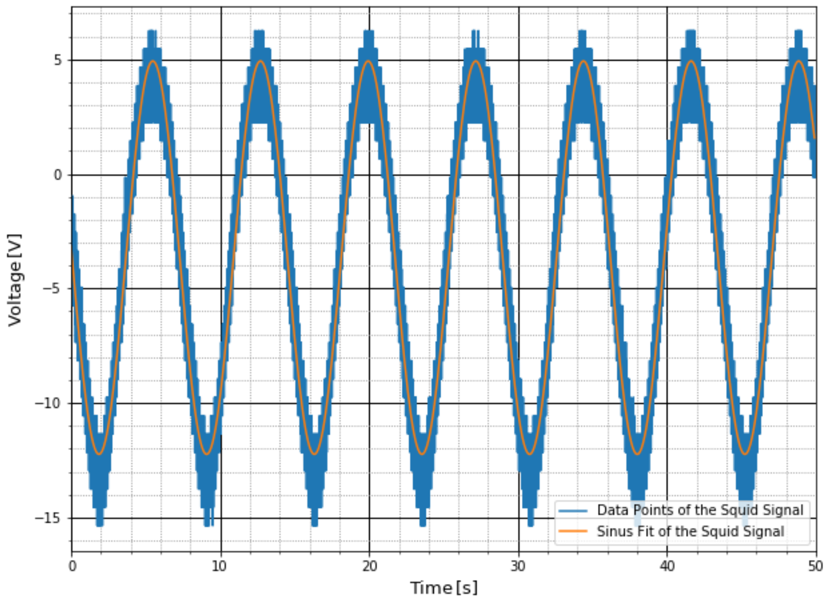

Figure 40: Plot of the SQUID signal with Magnet chips as a sample.

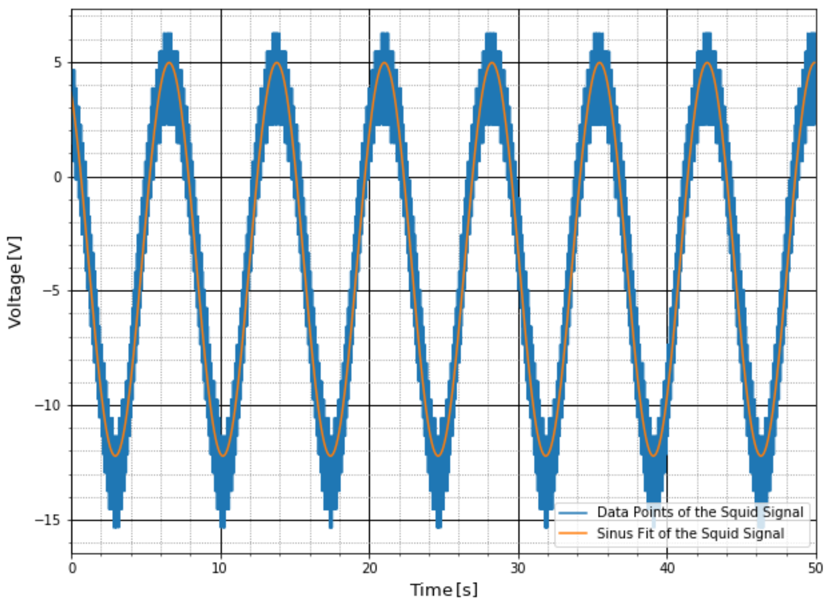

Figure 41: Plot of the SQUID signal with Magnet chips as a sample.

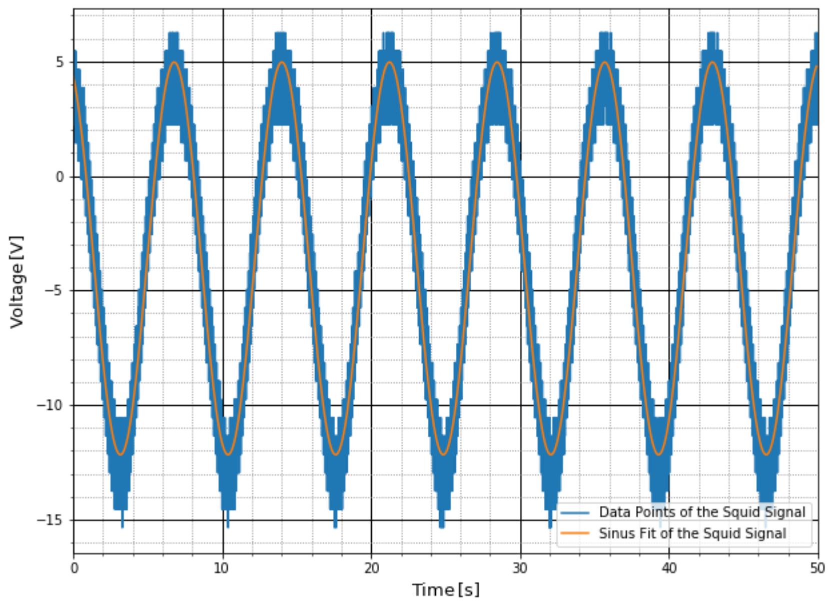

Figure 42: Plot of the SQUID signal with Magnet chips as a sample.

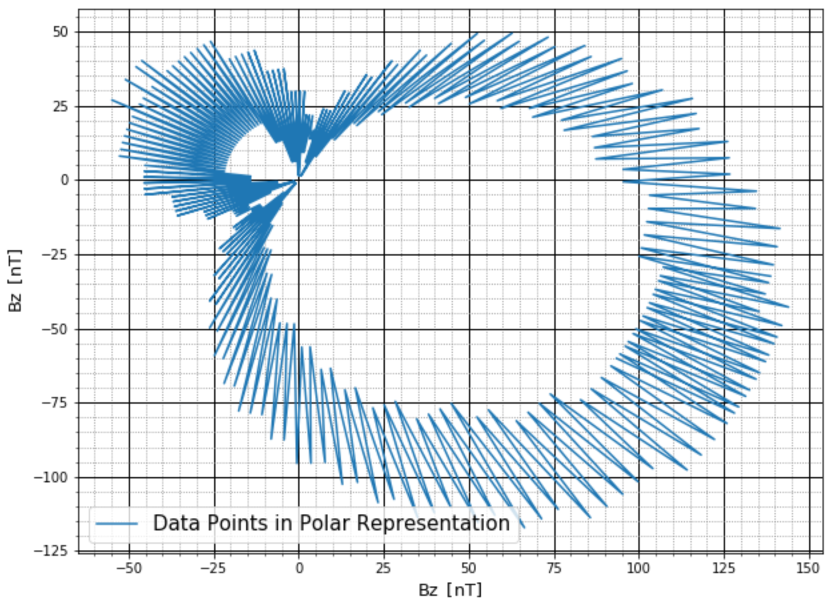

Figure 43: Polar Representation for one period of the signal coming from the magnet chips.

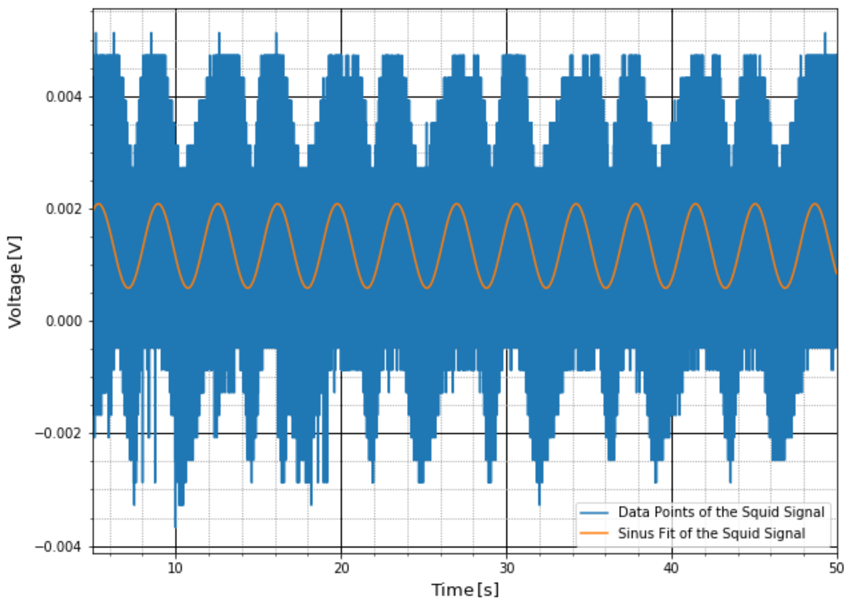

Figure 44: Plot of the SQUID signal with a stone as a sample.

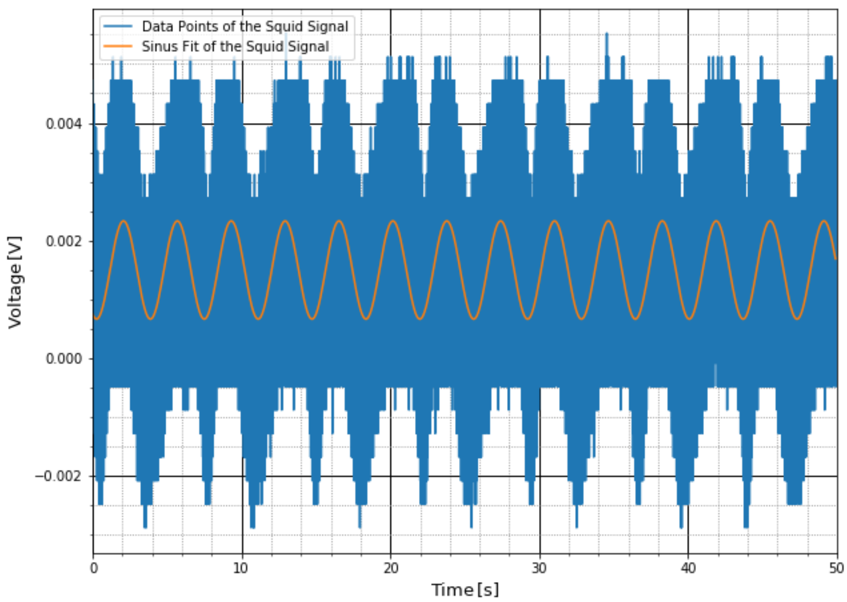

Figure 45: Plot of the SQUID signal with a stone as a sample.

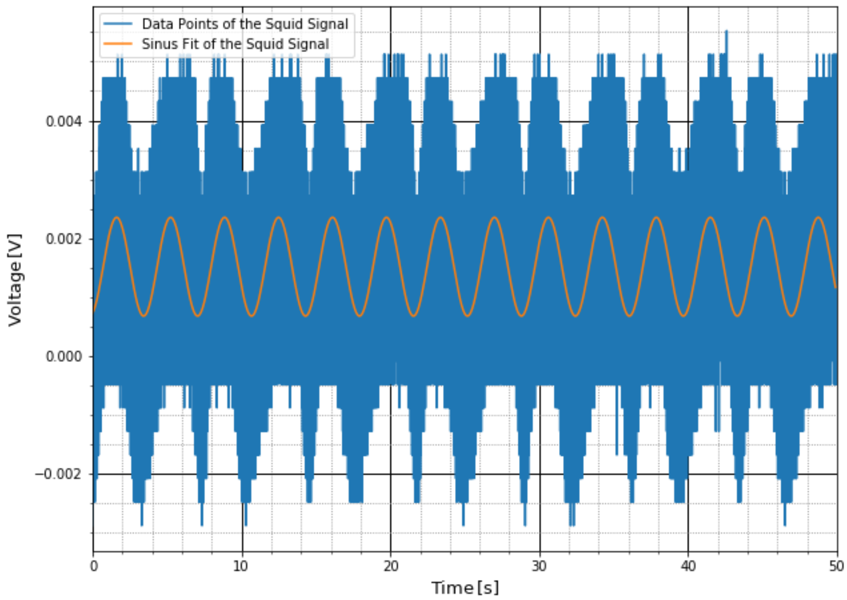

Figure 46: Plot of the SQUID signal with a stone as a sample.

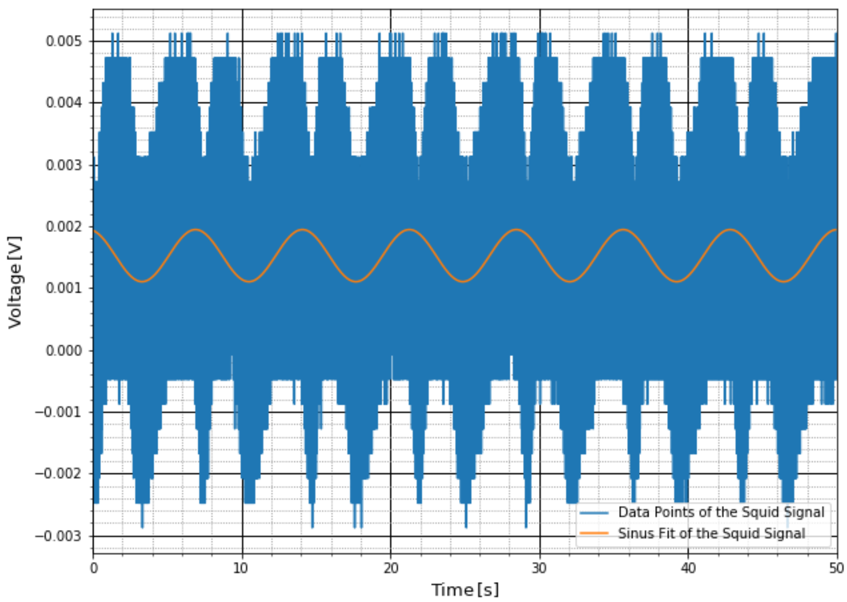

Figure 47: Plot of the SQUID signal with a Stone as a sample.

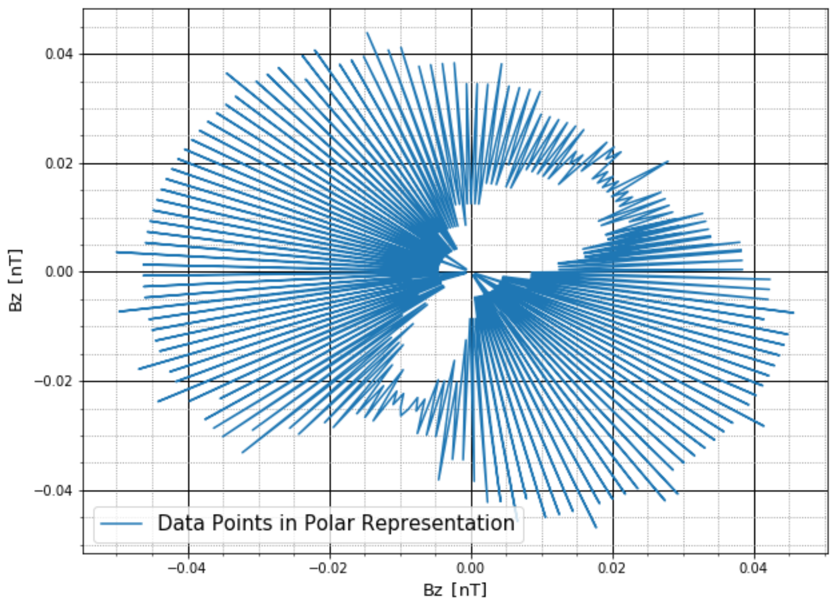

Figure 48: Polar Representation for one period of the signal coming from the stone.

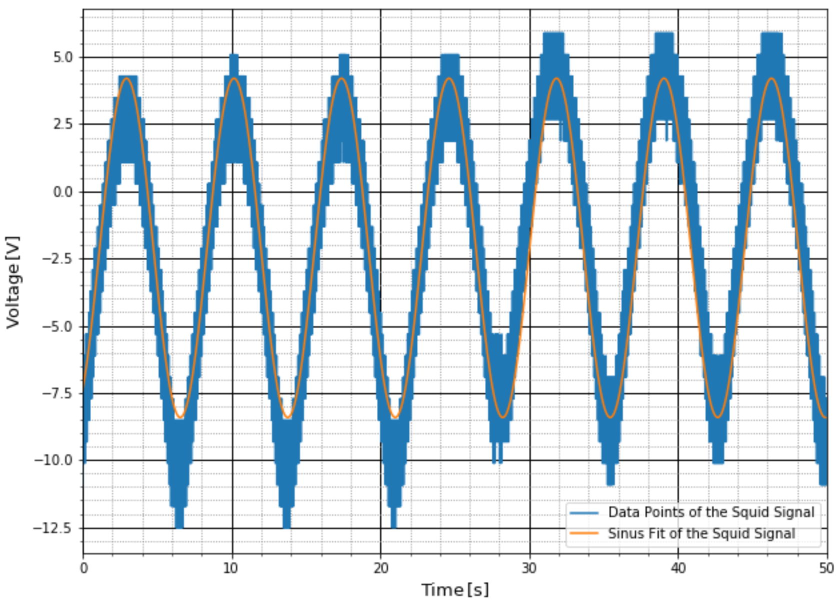

Figure 49: Plot of the SQUID signal with a magnet as a sample.

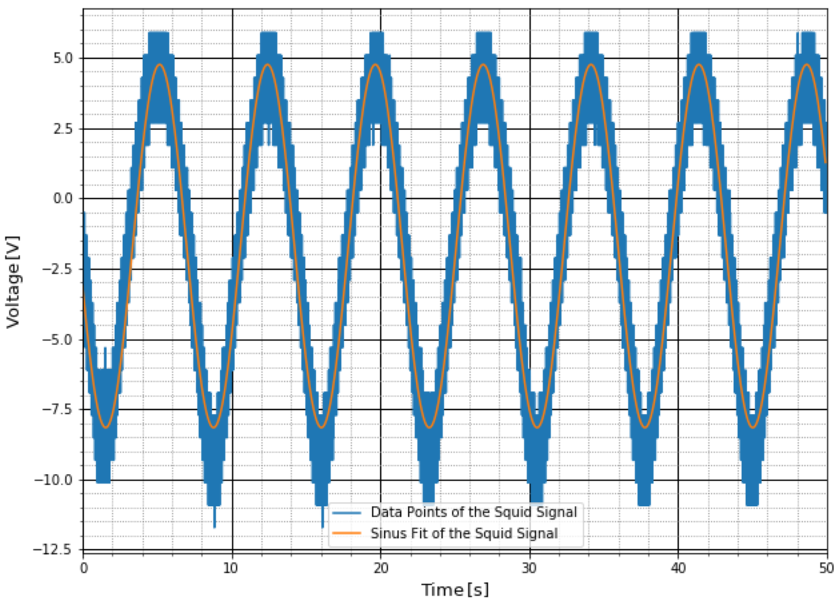

Figure 50: Plot of the SQUID signal with a magnet as a sample.

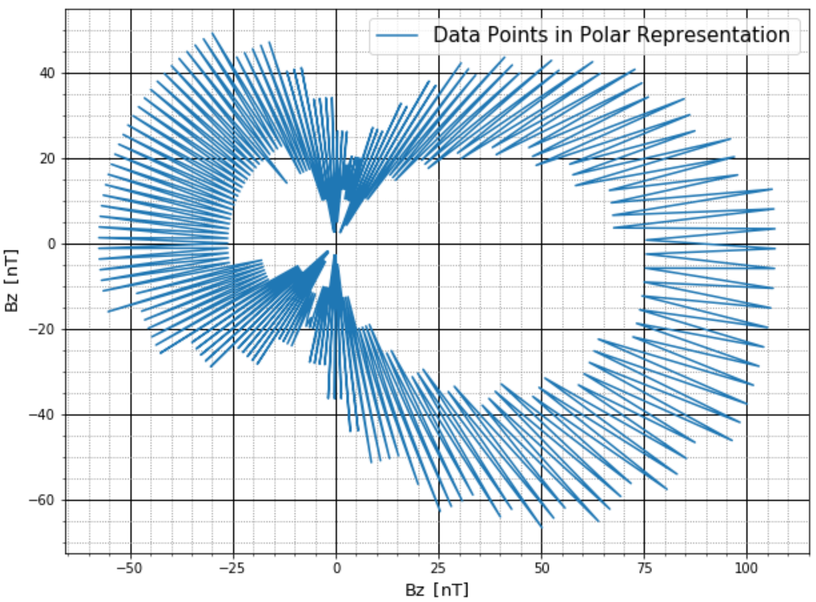

Figure 51: Polar Representation for one period of the signal coming from the magnet.